



Hypertensive Adults Exhibit Lower Myelin Content: A Multicomponent Relaxometry and Diffusion Magnetic Resonance Imaging Study

John P. Laporte, Mary E. Faulkner, Zhaoyuan Gong^{id}, Mohammad A.B.S. Akhonda, Luigi Ferrucci^{id}, Josephine M. Egan, Mustapha Bouhrara^{id}

BACKGROUND: It is unknown whether hypertension plays any role in cerebral myelination. To fill this knowledge gap, we studied 90 cognitively unimpaired adults, age range 40 to 94 years, who are participants in the Baltimore Longitudinal Study of Aging and the Genetic and Epigenetic Signatures of Translational Aging Laboratory Testing to look for potential associations between hypertension and cerebral myelin content across 14 white matter brain regions.

METHODS: Myelin content was probed using our advanced multicomponent magnetic resonance relaxometry method of myelin water fraction, a direct and specific magnetic resonance imaging measure of myelin content, and longitudinal and transverse relaxation rates ($R1$ and $R2$), 2 highly sensitive magnetic resonance imaging metrics of myelin content. We also applied diffusion tensor imaging magnetic resonance imaging to measure fractional anisotropy, mean diffusivity, radial diffusivity, and axial diffusivity values, which are metrics of cerebral microstructural tissue integrity, to provide context with previous magnetic resonance imaging findings.

RESULTS: After adjustment of age, sex, systolic blood pressure, smoking status, diabetes status, and cholesterol level, our results indicated that participants with hypertension exhibited lower myelin water fraction, fractional anisotropy, $R1$ and $R2$ values and higher mean diffusivity, radial diffusivity, and axial diffusivity values, indicating lower myelin content and higher impairment to the brain microstructure. These associations were significant across several white matter regions, particularly in the corpus callosum, fronto-occipital fasciculus, temporal lobes, internal capsules, and corona radiata.

CONCLUSIONS: These original findings suggest a direct association between myelin content and hypertension and form the basis for further investigations including longitudinal assessments of this relationship. (*Hypertension*. 2023;80:1728–1738. DOI: 10.1161/HYPERTENSIONAHA.123.21012.) • **Supplement Material.**

Key Words: diffusion tensor imaging ■ hypertension ■ magnetic resonance imaging ■ myelin water fraction ■ neurodegeneration

Hypertension is the primary risk factor for stroke, ischemic white matter lesions, infarcts, and atherosclerosis, as well as cardiovascular and microvascular diseases.^{1–3} Further, hypertension is the most widely accepted risk factor associated with a myriad of neurodegenerative diseases, especially Alzheimer's disease and related dementias.⁴ Emerging evidence suggests

that hypertension leads to vessel wall remodeling, potentially leading to hypoperfusion and associated hypoxia, as well as reduced glucose transport into the brain with concomitant accelerated cerebral tissue degeneration.^{5,6} Indeed, this paradigm is further supported by recent longitudinal studies revealing a direct association between hypertension in midlife and reduced cerebral blood flow

Correspondence to: Mustapha Bouhrara, Magnetic Resonance Physics of Aging and Dementia Unit, Laboratory of Clinical Investigation, National Institute on Aging (NIA), NIH, BRC 05C-222, 251 Bayview Blvd, Baltimore 21224, MD. Email bouhraram@mail.nih.gov

Supplemental Material is available at <https://www.ahajournals.org/doi/suppl/10.1161/HYPERTENSIONAHA.123.21012>.

For Sources of Funding and Disclosures, see page 1736.

© 2023 The Authors.

Hypertension is published on behalf of the American Heart Association, Inc., by Wolters Kluwer Health, Inc. This is an open access article under the terms of the [Creative Commons Attribution Non-Commercial-NoDerivs](https://creativecommons.org/licenses/by-nc-nd/4.0/) License, which permits use, distribution, and reproduction in any medium, provided that the original work is properly cited, the use is noncommercial, and no modifications or adaptations are made.

Hypertension is available at www.ahajournals.org/journal/hyp

NOVELTY AND RELEVANCE

What Is New?

This is the first study, to our knowledge, that explicitly investigated the association between hypertension and cerebral myelin content probed using a direct magnetic resonance imaging measure.

What Is Relevant?

In a healthy adult population, elevated blood pressure is associated with reduced cerebral white matter

tissue myelination. Further, patients under hypertension control medication still exhibit significantly lower myelin content as compared with control.

Clinical/Pathophysiological Implications?

This work lay the ground to future efforts to support myelin health in hypertension and examine the effect of hypertensive medications on mitigating myelin damage.

Nonstandard Abbreviations and Acronyms

AxD	axial diffusivity
bSSFP	balanced steady-state free precession
DAM	double angle method
DTI	diffusion tensor imaging
FA	fractional anisotropy
FSL	The FMRIB Software Library
MD	mean diffusivity
MRI	magnetic resonance imaging
MWF	myelin water fraction
R1	longitudinal relaxation rate
R2	transverse relaxation rate
RD	radial diffusivity
ROI	regions of interest
SPGR	spoiled gradient-recalled echo
TE	echo time
TR	repetition time

in later life.^{7,8} Therefore, examining the extent of any possible association between hypertension and cerebral tissue integrity is paramount for our global understanding of neurodegenerative disease risk factors and progression.

In recent years, magnetic resonance imaging (MRI) studies, based extensively on diffusion tensor imaging (DTI), have revealed an association between hypertension and abnormal cerebral microstructural white matter integrity.⁸ DTI is an MRI technique sensitive to the underlying microarchitecture of the brain parenchyma and the degree and direction of water molecule mobility. These studies have documented that hypertension, indicated by a blood pressure >140/90 mmHg or the use of anti-hypertensive medication, is associated with lower values of fractional anisotropy (FA) and higher values of mean diffusivity (MD), radial diffusivity (RD), and axial diffusivity (AxD).^{9–11} Reduced FA concomitant with an increase in RD is associated with demyelination,¹² whereas reduced FA in conjunction with increased AxD is believed to be

associated with axonal injury or death.¹³ These changes in cerebral microstructural integrity associated with hypertension have been interpreted as deterioration in axonal myelination. However, although DTI metrics such as FA and MD are sensitive to cerebral microstructural changes, they are not specific. Indeed, there are multiple methodological and biological factors that can affect the DTI-derived eigenvalues from which the DTI indices are calculated^{14,15}; these include, but not limited to, axonal degeneration, flow, temperature, hydration, macromolecular content and architectural features, including fiber fanning or crossing. Therefore, to our knowledge, the association between hypertension and myelination has not yet been established. To address this limitation, multicomponent relaxometry methods provide a greater specificity to quantify myelin content in white matter and probe related changes that occur during brain development and neurodegenerative diseases.^{16,17} Multicomponent relaxometry separates the measured MR signal in white matter into 2 pools of water, namely the intra- and extracellular water pool and the water trapped between the myelin sheaths calculated as the myelin water fraction (MWF).^{18,19} MWF is an in vivo specific index of myelin content and is a potential marker for myelin alterations. To the best of our knowledge, no MR studies have employed multicomponent relaxometry analysis, specifically MWF imaging, to investigate the relationship between myelin content and hypertension in aging adults.

In this study, we examined the association between hypertension and myelin content as probed using MWF on a cohort of well-characterized cognitively unimpaired adults ($N=90$), across the age range of 40 to 94 years. Each participant underwent our Bayesian Monte Carlo-mcDESPOT protocol for MWF as a direct measure of myelin content, as well as mapping of longitudinal and transverse relaxation rates ($R1$ and $R2$) as sensitive but nonspecific measures of myelin content.^{6,20–22} Indeed, $R1$ and $R2$ values depend on both water mobility and macromolecular tissue composition, including local lipid and iron content, the main constituents of myelin, and thus are expected to be directly associated with differences in

myelin content. To establish a connection with previous MRI findings, participants have undergone our additional DTI protocol for FA, MD, RD, and AxD mapping as well.²³

METHODS

Data Availability

The data that support the findings of this study are available from the corresponding author upon reasonable request.

Study Cohort

Participants are volunteers of the Baltimore Longitudinal Study of Aging (BLSA) and the Genetic and Epigenetic Signatures of Translational Aging Laboratory Testing (GESTALT) studies.^{24,25} Both BLSA and GESTALT seek to evaluate multiple biomarkers associated with aging, with essentially identical inclusion and exclusion criteria. Participants with metallic implants or major neurological or medical disorders are excluded on first admission. All participants were administered the Mini Mental State Examination (MMSE). Informed consent was obtained from participants before the conduct of the experiments, in compliance with the local Institutional Review Board.

Data Acquisition

MRI scans were performed on a 3T whole body Philips MRI system (Achieva, Best, The Netherlands) using the internal quadrature body coil for transmission and an 8-channel phased-array head coil for reception. Each participant underwent our Bayesian Monte Carlo-mcDESPOT protocol for MWF, $R1$, and $R2$ mapping.^{6,16,26,27} This imaging protocol consisted of 3D spoiled gradient-recalled echo (SPGR) images acquired with flip angles of [2 4 6 8 10 12 14 16 18 20]°, echo time (TE) of 1.37 ms, repetition time (TR) of 5 ms and acquisition time of ~5 minutes, as well as 3D balanced steady-state free precession (bSSFP) images acquired with flip angles of [2 4 7 11 16 24 32 40 50 60]°, TE of 2.8 ms, TR of 5.8 ms, and acquisition time of ~6 minutes. The bSSFP images were acquired with radiofrequency excitation pulse phase increments of 0 or 180° to account for off-resonance effects, with a total scan time of ~12 minutes (~6 minutes for each phase-cycling scan). All SPGR and bSSFP images were acquired with an acquisition matrix of 150×130×94, voxel size 1.6×1.6×1.6 mm. To correct for excitation radiofrequency inhomogeneity,^{28,29} we used the double-angle method (DAM), which consisted of acquiring 2 fast spin-echo images with flip angles of 45° and 90°, TE of 102 ms, TR of 3000 ms, acquisition voxel size of 2.6×2.6×4 mm, and acquisition time of ~4 minutes. The total acquisition time was ~21 minutes. All images were acquired with field-of-view of 240×208×150 mm, SENSE factor of 2, and reconstructed to a voxel size of 1×1×1 mm. We emphasize that all MRI studies and ancillary measurements were performed with the same MRI system, with the same pulse sequences, and at the same facility for both BLSA and GESTALT participants.

The DTI protocol consisted of diffusion-weighted images (DWIs) acquired with single-shot EPI, TR of 10 s, TE of 70 ms, 2 b -values of 0 and 700 s/mm², with the latter encoded in 32 directions, acquisition matrix of 120×104×75, and acquisition

voxel size of 2×2×2 mm. Two images at $b=0$ s/mm² were acquired and then averaged. All images were acquired with field-of-view of 240×208×150 mm.

Data Processing

For each participant, using the FLIRT analysis as implemented in the The FMRIB Software Library (FSL) software,³⁰ all SPGR, bSSFP, or DAM images were linearly registered to the SPGR image obtained at FA of 8° and the respective derived transformation matrices were then applied to the original SPGR, bSSFP, or DAM images. Then, a whole-brain MWF map was generated using Bayesian Monte Carlo-mcDESPOT from these co-registered SPGR, bSSFP, and DAM datasets.^{6,16,20} Bayesian Monte Carlo-mcDESPOT assumes a 2-relaxation time components system consisting of a short component, attributed to myelin water, and a long component, attributed to intra- and extracellular water. We used the signal model explicitly accounting for nonzero TE.^{6,16,20} This emerging method offers rapid and reliable whole-brain MWF map within feasible clinical time^{6,16,20,31–34} and has been used in assessing myelin loss in mild cognitive impairment and dementias, as well as examining factors influencing cerebral myelination in normative aging.^{16,22,23,26,32–45} A whole-brain $R1$ map was also generated from the co-registered SPGR and DAM datasets using DESPOT1,²¹ and a whole-brain $R2$ map was generated from the co-registered bSSFP and DAM datasets using DESPOT2.²¹ The DW images were corrected for eddy current using the function *eddy* in FSL and for motion effects using the affine registration tools as implemented in FSL³⁰ and registered to the DW image obtained with $b=0$ s/mm² using FNIRT. We used the DTIfit tool implemented in FSL to calculate the eigenvalue maps, which were used to calculate FA, RD, MD, and AxD.⁴⁶

Further, using FSL software,³⁰ the averaged SPGR image over flip angles underwent nonlinear registration to the Montreal Neurological Institute standard space, and the computed transformation matrix was then applied to the corresponding DTI indices, MWF, $R1$, and $R2$ maps. Fourteen white matter regions of interest (ROIs) were defined from the Montreal Neurological Institute structural atlas corresponding to the whole brain, the frontal, parietal, temporal, and occipital lobes, cerebellum, corpus callosum, internal capsule, cerebral peduncle, corona radiata, thalamic radiation, fronto-occipital fasciculus, longitudinal fasciculus, and forceps. ROIs were eroded to reduce partial volume effect. Within each ROI, the mean FA, RD, MD, AxD, MWF, $R1$, and $R2$ values were calculated.

Systolic and Diastolic Blood Pressures

Systolic blood pressure and diastolic blood pressure were recorded 3 times in both arms in a seated position using a mercury sphygmomanometer sized to the arm of each participant, and the mean of the systolic and diastolic measurements were used in the subsequent analyses.⁴⁷ Hypertension was defined as a systolic blood pressure greater than or equal to 140 mmHg, a diastolic blood pressure greater than or equal to 90 mmHg, or the use of prescription hypertension medications.

Statistical Analysis

To investigate the effect of hypertension on relaxometry (MWF, $R1$, $R2$) and diffusion (FA, MD, RD, AxD) MRI metrics, a multiple

linear regression analysis was applied using MWF, $R1$, $R2$, FA, MD, RD, or AxD within each ROI as the dependent variable and hypertension status, smoking status, systolic blood pressure, diabetes, cholesterol, age, and sex as independent variables. In all cases, the threshold for statistical significance was $P < 0.05$, while for close-to-significance was taken as $P < 0.1$ after correction for multiple ROI comparisons using the false discovery rate method.^{48,49} All calculations were performed with MATLAB software (MathWorks, Natick, MA).

RESULTS

Participants Demographic Characteristics

Demographic characteristics of the participants are shown in Table 1. After restricting the age range to participants of 40+ years and excluding 6 participants with either cognitive impairment, missing data or bad quality images due to severe motion artifacts, the final cohort consisted of 90 cognitively unimpaired volunteers (mean \pm SD MMSE=28.8 \pm 1.3) ranging in age from 40 to 94 years (64.6 \pm 17.1 years). Of this cohort, 49 (54.4%) were men, 30 (33.3%) were identified as cigarette smokers while 59 (65.6%) as nonsmokers. Among the cohort, 27 were hypertensive (30.0%), 23 of which taking antihypertensive medication. This cohort also included 3 participants (3.3%) with diabetes (2 of them were hypertensive), while 87 participants were nondiabetic (96.7%). The mean \pm SD values of the systolic blood pressure and diastolic blood pressure were 117.6 \pm 14.5 and 68.5 \pm 8.6, respectively,

and the mean \pm SD values of cholesterol level were 183.0 \pm 35.1. Stratification of this cohort into hypertensive and control groups showed that, compared to the control group, the hypertensive group exhibits significantly ($P < 0.05$) higher mean values of age and systolic blood pressure but a significantly ($P < 0.05$) lower mean value of cholesterol level. The mean diastolic blood pressure was not significantly ($P > 0.1$) different between the 2 groups.

Associations Between Hypertension and Cerebral Microstructure

Figure 1 shows the MWF, $R1$ and $R2$ relaxometry parameter maps of either hypertensive or nonhypertensive participants within an age range of 70 to 94 years. This limited age range minimizes the potential effect of age on derived MR parameter maps for this qualitative analysis (statistical quantification of the effect of age as a covariate will be presented below [Tables 2 and 3]). Visual inspection indicates that, overall, hypertensive participants exhibit lower regional MWF, $R1$ and $R2$ values as compared with nonhypertensive participants. These qualitative results suggest a potentially strong association between hypertension and myelin content.

Similarly, Figure 2 shows the FA, MD, RD, and AxD DTI parameter maps of either hypertensive or nonhypertensive participants within an age range of 70 to 94 years. Again, this limited age range is used to minimize the potential effect of age on derived DTI parameter

Table 1. Demographic Characteristics of Participants of the Study Cohort

	Full cohort	Hypertensive	Nonhypertensive
Sample size	N=90	n=27 (30.0%)	n=63 (70.0%)
Age, y; mean \pm SD (min–max)	64.6 \pm 17.1 (40–94)	76.0 \pm 14.1* (41–94)	59.7 \pm 15.9* (40–94)
Sex			
Male, N (%)	49 (54.4%)	15 (55.6%)	34 (54.0%)
Female, N (%)	41 (45.6%)	12 (44.4%)	29 (46.0%)
Smoker			
Smokers, N (%)	30 (33.3%)	12 (44.4%)	18 (28.6%)
Nonsmokers, N (%)	59 (65.6%)	15 (55.6%)	44 (69.8%)
Other, N (%)	1 (1.1%)	0 (0.0%)	1 (1.6%)
Diabetes			
Diabetic, N (%)	3 (3.3%)	2 (7.4%)	1 (1.6%)
Nondiabetic, N (%)	87 (96.7%)	25 (92.6%)	62 (98.4%)
SBP, mm Hg; mean \pm SD (min–max)	117.6 \pm 14.5 (89–161)	125.7 \pm 15.7* (106–161)	114.2 \pm 12.7* (89–139)
DBP, mm Hg; mean \pm SD (min–max)	68.5 \pm 8.6 (50–87)	66.4 \pm 9.8 (50–87)	69.3 \pm 8.0 (50–86)
Cholesterol, mean \pm SD (min–max)	183.0 \pm 35.1 (116–270)	169.7 \pm 37.8* (120–270)	188.7 \pm 32.5* (116–265)

DBP indicates diastolic blood pressure; max, maximum; min, minimum; and SBP, systolic blood pressure.

*Significant mean difference ($P < 0.05$) between the hypertensive and the control groups.

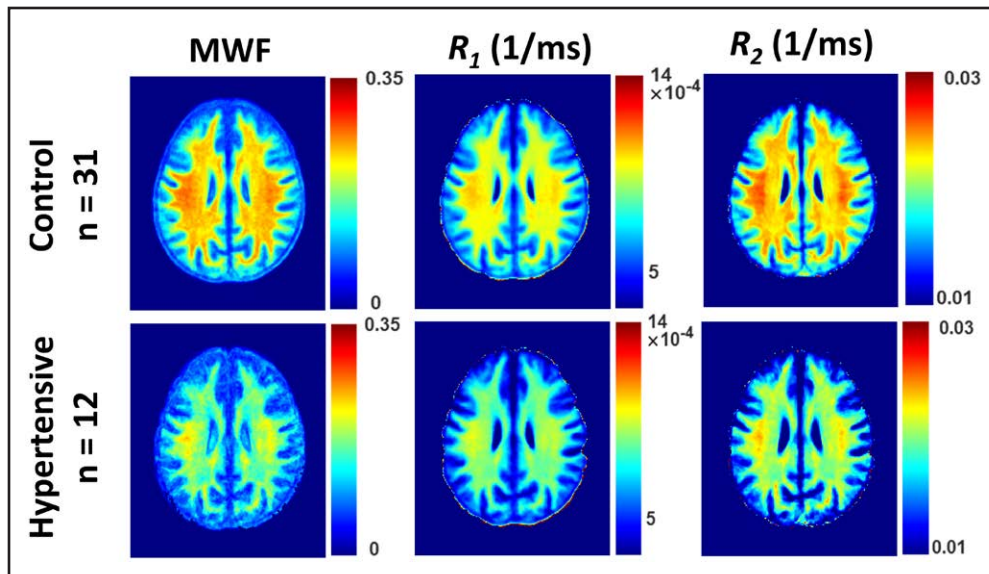


Figure 1. Examples of myelin water fraction (MWF), R_1 and R_2 parameter maps averaged across participants drawn from a limited age range (70–94 years) either hypertensive ($n=12$) or nonhypertensive ($n=31$) to mitigate the effect of age.

Results are shown for a representative slice. Visual inspection indicates that overall hypertensive patients exhibit lower regional MWF, R_1 and R_2 values, as compared with controls. R_1 indicates longitudinal relaxation rate; and R_2 , transverse relaxation rate.

maps for this qualitative analysis. Visual inspection indicates that, overall, hypertensive participants exhibit lower FA and higher MD, RD, and AxD values. In other words, hypertension is associated with higher diffusivities and a lower level of water diffusion. These qualitative results provide further support that hypertension is associated with reduced microstructural white matter integrity.

Table 2 summarizes the results of the multiple regression analysis of MWF, R_1 and R_2 versus hypertension and age in 14 white matter ROIs. In agreement with Figure 1, there are significant ($P<0.05$), or close-to-significant ($P<0.1$), negative correlations after false discovery rate correction, between hypertension and MWF or R_2 in all regions but the cerebellum and cerebral peduncles, and between hypertension and R_1 in all regions but the cerebellum. This is clearly seen in Figure 3 indicating that the hypertensive patients exhibit lower parameter values as compared with the control group. It was also found that the corpus callosum and the corona radiata exhibited the steepest slopes in the correlations between hypertension and MWF, R_1 and R_2 . Furthermore, as expected, age was found to be a significant covariate with hypertension and exhibited negative slopes with respect to all metrics except for R_1 in the cerebral peduncles (Table 2; Figure 3). Finally, the regression results for all the independent parameters included in the regression model are shown in the [Supplemental Material](#).

Table 3 summarizes the results of the multiple regression analysis of FA, MD, RD, and AxD versus hypertension and age in the 14 white matter ROIs studied after controlling for relevant covariates. There are significant ($P<0.05$), or close-to-significant ($P<0.1$), negative correlations after false discovery rate correction, between

FA and hypertension and positive correlations with MD, RD, and AxD in most ROIs investigated. Examples of these association are illustrated shown in Figure 3. Here, we found that the steepest slopes in the correlation between hypertension and FA, MD, RD, and AxD were found in the temporal lobe, fronto-occipital fasciculus, and the internal capsules. We note that in contrast to the results of the multicomponent relaxometry analysis, less ROIs were found to be statistically significant between hypertensive and control groups, with the parietal lobe and forceps regions found to be insignificant in the correlation between hypertension and diffusivity metrics. However, the overall trend of the data follows the paradigm of impaired white matter microstructural integrity. Furthermore, in all ROIs investigated, the effect of age was found to be significant with respect to all metrics (Table 3; Figure 3). Finally, the regression results for all the independent parameters included in the regression model are shown in the [Supplemental Material](#).

DISCUSSION

In this MRI study, using advanced multicomponent relaxometry and DTI analyses for both direct and indirect measurements of myelin content, we found that the hypertension status is associated with lower regional myelin content as measured by the MWF, R_1 , R_2 , and DTI metrics (FA, MD, RD, and AxD). These regional associations were observed in a cohort of well-characterized, cognitively unimpaired, adults. These results provide further evidence of the association between a well-known cardiovascular risk factor, specifically hypertension, and cerebral white matter tissue integrity in the absence of

Table 2. Regression Coefficient (β), Including SE, and Significance (P Value After FDR) of Relaxometry Metrics (MWF, R_1 , and R_2) Versus Hypertension and Age Across 14 WM ROIs

ROIs	MWF		R_1		R_2	
	Hypertension	Age	Hypertension	Age	Hypertension	Age
	β (SE) $\times 10^{-2}$	β (SE) $\times 10^{-4}$	β (SE) $\times 10^{-5}$	β (SE) $\times 10^{-6}$	β (SE) $\times 10^{-3}$	β (SE) $\times 10^{-5}$
WB	-1.97 (0.68)	-9.64 (1.76)	-5.76 (1.74)	-1.71 (0.45)	-1.20 (0.46)	-6.12 (1.17)
	0.010*	<0.001*	0.004*	<0.001*	0.021*	<0.001*
FL	-2.43 (0.67)	-11.2 (1.73)	-6.77 (1.61)	-2.06 (0.41)	-1.45 (0.45)	-6.95 (1.15)
	0.006*	<0.001*	0.001*	<0.001*	0.009*	<0.001*
OL	-1.55 (0.87)	-8.43 (2.23)	-4.18 (1.98)	-1.41 (0.51)	-1.19 (0.57)	-5.61 (1.47)
	0.090*	<0.001*	0.043*	0.008*	0.052*	<0.001*
PL	-2.41 (0.78)	-10.1 (2.00)	-6.05 (1.75)	-1.87 (0.45)	-1.35 (0.53)	-7.06 (1.37)
	0.010*	<0.001*	0.003*	<0.001*	0.021*	<0.001*
TL	-1.84 (0.82)	-9.28 (2.10)	-4.91 (1.83)	-1.77 (0.47)	-1.28 (0.54)	-5.55 (1.38)
	0.038*	<0.001*	0.011*	<0.001*	0.027*	<0.001*
CRB	-0.50 (0.73)	-6.70 (1.89)	-2.63 (1.78)	-1.09 (0.46)	-0.20 (0.51)	-4.71 (1.30)
	0.500*	<0.001*	0.145*	0.021*	0.693*	<0.001*
CC	-2.06 (0.69)	-9.01 (1.77)	-7.41 (1.82)	-1.90 (0.47)	-1.72 (0.55)	-6.78 (1.42)
	0.010*	<0.001*	0.001*	<0.001*	0.009*	<0.001*
IC	-1.40 (0.71)	-9.61 (1.83)	-4.91 (1.74)	-1.77 (0.45)	-0.84 (0.43)	-5.48 (1.11)
	0.067*	<0.001*	0.008*	<0.001*	0.065*	<0.001*
CR	-3.03 (0.88)	-11.8 (2.27)	-7.79 (1.93)	-2.16 (0.50)	-1.71 (0.53)	-5.84 (1.37)
	0.006*	<0.001*	0.001*	<0.001*	0.009*	<0.001*
CP	-0.70 (0.63)	-4.07 (1.61)	-3.70 (1.77)	-0.50 (0.46)	-0.31 (0.48)	-3.54 (1.23)
	0.285*	0.013*	0.043*	0.273*	0.561*	<0.001*
TR	-2.20 (0.83)	-10.1 (2.14)	-5.70 (1.88)	-2.04 (0.48)	-1.38 (0.53)	-5.34 (1.37)
	0.015*	<0.001*	0.006*	<0.001*	0.021*	0.005*
FOF	-2.37 (0.77)	-10.7 (1.98)	-5.95 (1.85)	-2.09 (0.48)	-1.52 (0.51)	-6.71 (1.30)
	0.010*	<0.001*	0.004*	<0.001*	0.010*	<0.001*
LF	-2.28 (0.80)	-9.92 (2.06)	-5.63 (1.88)	-2.02 (0.49)	-1.29 (0.50)	-5.35 (1.29)
	0.010*	<0.001*	0.006*	<0.001*	0.021*	<0.001*
Fr	-2.24 (0.76)	-10.6 (1.95)	-6.12 (1.87)	-2.02 (0.48)	-1.57 (0.51)	-6.38 (1.30)
	0.010*	<0.001*	0.004*	<0.001*	0.009*	<0.001*

The multiple regression model is given by: $MRI \sim \beta_0 + \beta_{age} \times age + \beta_{Hypertension} \times Hypertension + \beta_{Smoking} \times Smoking + \beta_{SBP} \times SBP + \beta_{sex} \times sex + \beta_{Diabetes} \times Diabetes + \beta_{Cholesterol} \times Cholesterol$, where MRI corresponds to MWF, R_1 , or R_2 . The regression model accounted for sex, smoking status, diabetes status and hypertension as categorical variables. CC indicates corpus callosum; CR, corona radiata; CRB, cerebellum; FDR, false discovery rate; FL, frontal lobe; FOF, fronto-occipital fasciculus; Fr, forceps; IC, internal capsule; LF, longitudinal fasciculus; MRI, magnetic resonance imaging; MWF, myelin water fraction; OL, occipital lobe; PL, parietal lobe; R_1 , Longitudinal rate of relaxation; R_2 , Transverse rate of relaxation; ROI, region-of-interest; SBP, systolic blood pressure; SE, standard error; TL, temporal lobe; TR, thalamic radiation; WB, whole brain; and WM, white matter.

* P value indicates statistical significance ($P < 0.05$) or close-to-significance ($P < 0.1$), after FDR correction. We note that the regression results for all the independent parameters included in the regression model are shown in the Tables S1 through S3.

cognitive impairment. Furthermore, to our knowledge, this is the first investigation to indicate a direct association between hypertension and myelin deterioration, as measured by a specific proxy of myelin content (ie, MWF). In our analysis, we found that hypertension was associated with higher MD, RD, and AxD values and lower MWF, FA, R_1 , and R_2 values. Our DTI results agree with previous DTI studies that have also shown a connection between cardiovascular risk factors, especially hypertension, and decreased cerebral microstructural integrity.^{9–12,50–52}

While our relaxometry results, in conjunction with our DTI results, do not prove causality, they support

the paradigm that hypertension impairs white matter microstructural integrity, especially the myelination process.^{5,53} Indeed, studies have revealed association between increased arterial stiffness and hypertension during the aging process.^{54–56} One of these paradigms suggests that vascular dysregulation due to potential synergetic effects of arterial remodeling and blood pressure may lead to transient reductions in cerebral blood flow, consequently resulting in transient decreased glucose transport into brain and hypoxia, and concomitant myelin injury.³⁵ Indeed, recent works have demonstrated that deficits in cerebral blood flow are directly linked to

Table 3. Regression Coefficient (β), Including SE, and Significance (P value After FDR) of Diffusion Tensor Imaging metrics (FA, MD, RD, and AxD) Versus Hypertension and Age Across 14 WM ROIs

ROI	FA		MD		RD		AxD	
	Hypertension	Age	Hypertension	Age	Hypertension	Age	Hypertension	Age
	β (SE) $\times 10^{-2}$	β (SE) $\times 10^{-4}$	β (SE) $\times 10^{-5}$	β (SE) $\times 10^{-6}$	β (SE) $\times 10^{-5}$	β (SE) $\times 10^{-6}$	β (SE) $\times 10^{-5}$	β (SE) $\times 10^{-6}$
WB	-1.20 (0.53)	-6.87 (1.36)	1.68 (1.47)	2.46 (0.38)	2.62 (1.60)	2.87 (0.41)	3.07 (1.70)	3.06 (0.43)
	0.041*	<0.001*	0.276	<0.001*	0.122	<0.001*	0.086*	<0.001*
FL	-2.51 (0.51)	-8.65 (1.31)	2.77 (1.67)	3.92 (0.43)	4.29 (1.76)	4.34 (0.45)	5.01 (1.83)	4.54 (0.47)
	<0.001*	<0.001*	0.128	<0.001*	0.026*	<0.001*	0.012*	<0.001*
OL	-1.81 (0.56)	-10.3 (1.44)	2.99 (0.91)	2.03 (0.23)	3.99 (1.13)	2.75 (0.29)	4.47 (1.29)	3.11 (0.33)
	0.006*	<0.001*	0.021*	<0.001*	0.002*	<0.001*	0.003*	<0.001*
PL	-1.08 (0.78)	-5.02 (2.00)	2.21 (1.52)	0.67 (0.39)	1.84 (1.46)	1.03 (0.37)	1.61 (1.59)	1.21 (0.41)
	0.168	0.015*	0.175	0.089*	0.229	0.004*	0.336	0.004*
TL	-5.52 (1.36)	-19.3 (3.49)	5.67 (2.12)	2.23 (0.54)	10.1 (2.60)	3.75 (0.67)	12.3 (3.16)	4.43 (0.81)
	<0.001*	<0.001*	0.032*	<0.001*	0.002*	<0.001*	0.002*	<0.001*
CRB	-2.50 (1.14)	-7.99 (2.93)	4.55 (2.01)	2.95 (0.52)	5.21 (2.17)	2.40 (0.56)	5.54 (2.36)	2.10 (0.60)
	0.044*	0.009*	0.042*	<0.001*	0.026*	<0.001*	0.030*	<0.001*
CC	-1.87 (0.70)	-11.8 (1.79)	5.79 (2.02)	1.98 (0.52)	6.10 (1.85)	2.42 (0.47)	6.27 (1.83)	2.62 (0.47)
	0.021*	<0.001*	0.030*	<0.001*	0.004*	<0.001*	0.003*	<0.001*
IC	-2.60 (1.14)	-6.35 (2.93)	4.05 (1.80)	2.34 (0.46)	6.02 (1.90)	2.33 (0.49)	7.07 (2.22)	2.27 (0.57)
	0.041*	0.033*	0.042*	<0.001*	0.005*	<0.001*	0.004*	<0.001*
CR	-2.04 (0.64)	-10.4 (1.64)	2.97 (1.21)	1.32 (0.31)	4.27 (1.21)	1.84 (0.31)	4.90 (1.30)	2.09 (0.33)
	0.006*	<0.001*	0.037*	<0.001*	0.002*	<0.001*	0.002*	<0.001*
CP	-1.64 (0.92)	-7.91 (2.35)	5.01 (1.78)	2.45 (0.46)	5.30 (1.78)	2.49 (0.46)	5.36 (1.91)	2.52 (0.49)
	0.091*	0.001*	0.030*	<0.001*	0.007*	<0.001*	0.011*	<0.001*
TR	-1.76 (0.77)	-6.86 (1.98)	2.82 (1.11)	1.11 (0.28)	3.76 (1.06)	1.41 (0.27)	4.22 (1.22)	1.56 (0.31)
	0.041*	0.001*	0.036*	<0.001*	0.002*	<0.001*	0.003*	<0.001*
FOF	-3.24 (0.90)	-15.0 (2.29)	3.52 (1.56)	1.36 (0.40)	6.11 (1.94)	2.60 (0.50)	7.40 (2.21)	3.21 (0.57)
	0.002*	<0.001*	0.042*	0.001*	0.005*	<0.001*	0.003*	<0.001*
LF	-6.49 (0.34)	-7.54 (0.87)	3.75 (2.14)	6.10 (0.55)	3.86 (2.13)	6.35 (0.55)	3.87 (2.14)	6.47 (0.55)
	0.074*	<0.001*	0.119	<0.001*	0.094*	<0.001*	0.086*	<0.001*
Fr	-6.92 (0.45)	-8.91 (1.15)	2.16 (2.98)	7.84 (0.76)	2.24 (3.02)	8.21 (0.77)	2.23 (3.05)	8.41 (0.78)
	0.136	<0.001*	0.470	<0.001*	0.460	<0.001*	0.465	<0.001*

The multiple regression model is given by: $MRI \sim \beta_0 + \beta_{age} \times age + \beta_{hypertension} \times Hypertension + \beta_{smoking} \times Smoking + \beta_{SBP} \times SBP + \beta_{sex} \times sex + \beta_{diabetes} \times Diabetes + \beta_{cholesterol} \times C$ holesterol, where MRI corresponds to FA, MD, RD, and AxD. The regression model accounted for sex, smoking status, diabetes status, and hypertension as categorical variables. AxD indicates axial diffusivity; CC, corpus callosum; CR, corona radiata; CRB, cerebellum; FA, fractional anisotropy; FDR, false discovery rate; FL, frontal lobe; FOF, fronto-occipital fasciculus; Fr, forceps; IC, internal capsule; LF, longitudinal fasciculus; MD, medial diffusivity; OL, occipital lobe; PL, parietal lobe; RD, radial diffusivity; ROI, region-of-interest; SBP, systolic blood pressure; SE, standard error; TL, temporal lobe; TR, thalamic radiation; WB, whole brain; and WM, white matter.

* P value indicates statistical significance ($P < 0.05$) or close-to-significance ($P < 0.1$), after FDR correction. We note that the regression results for all the independent parameters included in the regression model are shown in the [Tables S4 through S7](#).

reductions in cerebral tissue integrity. This association is present to a greater extent with white matter tissue damage.^{26,41,57} In fact, myelin maintenance through oligodendrocyte metabolism is an energy-demanding process, and therefore myelin homeostasis is particularly sensitive to hypoperfusion and consequent hypoxia or lack of essential nutrients for myelin synthesis.^{58,59} Recent *in vitro* studies have shown that oligodendrocytes are substantially more vulnerable to hypoxia and reduced supply of substrates that provide energy as can occur from hypoperfusion, when compared with other glial cells such as microglia and astroglia.⁶⁰ Furthermore, it has been shown that hypertension also interferes with

perivascular glymphatic drainage and blood-brain permeability. This would result in reduced drainage of toxic metabolites that adversely impact oligodendrocytes, the main cells synthesizing and maintaining myelin in the brain.⁶¹ Finally, interruption in the myelination process could result from chronic inflammation. Indeed, animal studies have demonstrated that chronically elevated blood pressure leads to adverse glial activation and increased brain inflammatory mediators that can be harmful to the myelin sheets and the normal functioning of oligodendrocyte cells.⁶² Nevertheless, despite these potential plausible mechanisms, further studies, especially of a longitudinal nature, are still required to

shed light on the association between blood pressure and myelination.

We found the steepest slopes in the correlations between hypertension and MWF, $R1$ and $R2$, in the corpus callosum, fronto-occipital fasciculus and corona radiata cerebral regions (Table 2). Numerous studies have found that these brain regions are particularly susceptible to microstructural damages due to elevated blood pressure.^{63–65} Interestingly, these brain structures have also been shown to exhibit higher sensitivity to the cerebral blood supply.^{12,20,66,67} For example, the corpus callosum has an especially high level of metabolic demand, receiving blood from the anterior communicating, anterior pericallosal, and posterior cerebral arteries.⁶⁸ Although ischemia in this region is rare due to the trifurcated nature of the vascular pathway, the energy-demanding process of myelination could be impeded from even minor changes in blood flow, such as those that occur from hypertension.^{69,70} However, it should be emphasized that the corpus callosum and the fronto-occipital fasciculus and corona radiata cerebral regions exhibit uniform myelination throughout their structures which may have led to better detection of the association between hypertension and myelination.

Longitudinal studies have found that antihypertensive medication has a protective effect on the brain and helps to reduce the rate of cognitive decline and neurodegeneration, including in Alzheimer's disease.^{71,72} These studies consistently find that elevated blood pressure in midlife is more closely associated with

cognitive decline when compared with elevated blood pressure in late life.^{73,74} This could possibly be due to the slow progression of hypertensive arterial remodeling eventually leading to reduced blood flow post-ischemia.⁵ Interestingly, among the 27 hypertensive subjects in our study, 23 subjects were taking antihypertensive medication at the time of the scan. Although it is unclear whether the antihypertensive medication had some level of a protective effect on these participants, it is interesting to note that participants undergoing treatment still had significantly lower myelin content or higher microstructural damage in many of the regions analyzed (Table 1). We conjecture that this may be due to either microstructural damage being done before the treatment of the antihypertensive medication or as a demonstration of the possible limitations of the antihypertensive medication on protecting the overall cerebral microstructure long term (Figures 1 and 2). Unfortunately, the information regarding the duration under medication was not available to further explore these interesting aspects including the effect of medication duration on myelination.

Although our investigation examined a relatively large cohort and used advanced MRI methodology to probe myelin content and obtain diffusion metrics, our work has certain limitations. The cross-sectional nature of the study precludes us from drawing any causal link between hypertension and demyelination; future longitudinal studies are needed to further support this potential association. We also note that the causal

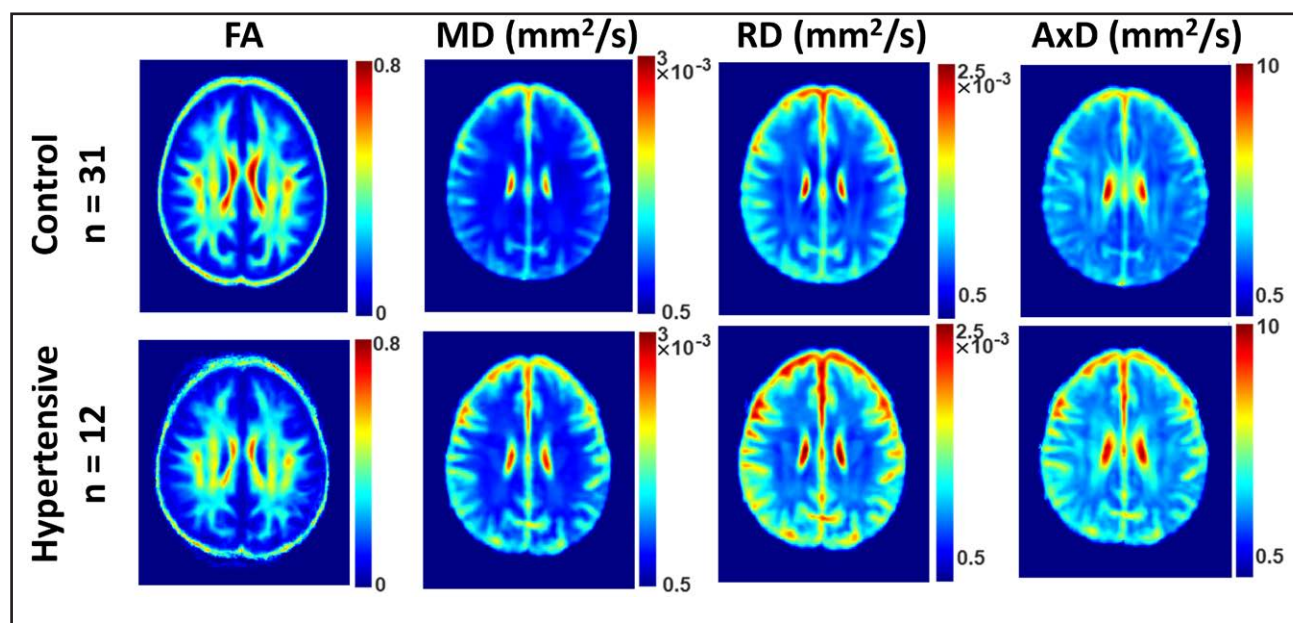


Figure 2. Examples of fractional anisotropy (FA), medial diffusivity (MD), radial diffusivity (RD), and axial diffusivity (AxD) parameter maps averaged across participants drawn from a limited age range (70–94 years) either hypertensive ($n=12$) or nonhypertensive ($n=31$) to mitigate the effect of age.

Results are shown for a representative slice. Visual inspection indicates that, overall, hypertensive participants exhibit lower FA and higher MD, RD, and AxD.

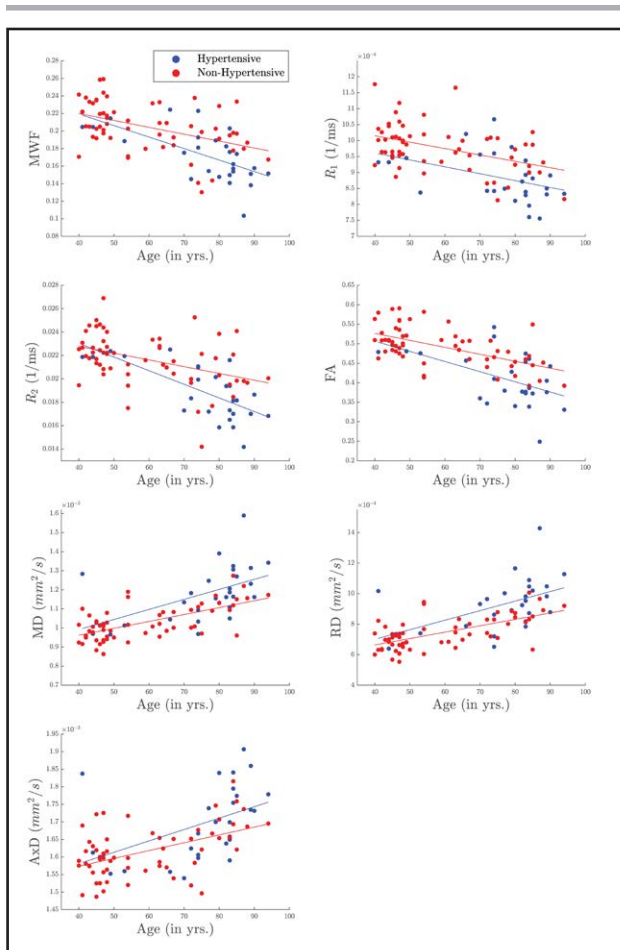


Figure 3. Examples of scatter plots of myelin water fraction (MWF), R_1 , R_2 , fractional anisotropy (FA), medial diffusivity (MD), radial diffusivity (RD), and axial diffusivity (AxD) as a function of age stratified by groups.

The hypertensive group is indicated by the blue color while the control group is indicated by the red color. Results were obtained from the corpus callosum ROI for MWF, R_1 and R_2 , while from the temporal lobes ROIs for FA, MD, RD, and AxD. It is readily seen that derived MWF, R_1 , R_2 , and FA parameter values decrease with age while the diffusivity values increase with age, as expected. Importantly, the hypertensive patients exhibit lower MWF, R_1 , R_2 , and FA parameter values or higher diffusivity values as compared to control. R_1 indicates longitudinal relaxation rate; and R_2 , transverse relaxation rate.

relationship between hypertension and myelination is difficult to determine as hypertension commonly occurs concomitant with many other cardiovascular risk factors, and we cannot control for all of them in our limited multiple linear regression model given the cohort size. Finally, determination of MR parameters can be biased due to several biological and methodological factors. These include, but are not limited to, the effects of magnetization transfer between macromolecules and free water protons, exchange between water pools, J-coupling, off-resonance, spin locking effects, water diffusion within different compartments, flow, temperature, hydration, internal gradients, and architectural features,

including fiber fanning or crossing.⁵⁷ Moreover, while the local distortions and motion artefacts in the DW images were corrected, we used the original b-vectors used in the acquisition. This could have introduced some bias in derived DTI indices. Finally, we did not control for white matter hyperintensity. Our inspection of this dataset revealed that white matter hyperintensities were limited to only a few subjects. This was expected given the very healthy nature of the BLSA and GESTALT cohorts. Further, the white matter hyperintensities were limited to small areas in the brain so that their impact in derived parameter values is negligible given the very large ROIs used in this study.

Perspectives

This study provides new insights into the association between hypertension and axonal demyelination among cognitively normal individuals spanning a wide age range. This work motivates further investigations to elucidate the extent to which hypertension and myelination are related in the pathological progression of neurodegenerative diseases, including in Alzheimer's disease and dementias. This study will provide guidance towards new targets for intervention through re-enforcing myelination and controlling blood pressure.

ARTICLE INFORMATION

Received January 30, 2023; accepted May 11, 2023.

Affiliation

Laboratory of Clinical Investigation (J.P.L., M.E.F., Z.G., M.A.B.S.A., J.M.E., M.B.) and Translational Gerontology Branch (L.F.), National Institute on Aging, National Institutes of Health, Baltimore, MD.

Acknowledgment

We thank Christopher Bergeron and Dr Linda Zukley for their help with data acquisition and logistics. We are also grateful to the participants of this study.

Sources of Funding

This research was supported entirely by the Intramural research Program of the National Institutes of Health, National Institute on Aging.

Disclosures

None.

REFERENCES

1. Wajngarten M, Silva GS. Hypertension and stroke: update on treatment. *Eur Cardiol.* 2019;14:111–115. doi: 10.15420/ecr.2019.11.1
2. Kokubo Y, Iwashima Y. Higher blood pressure as a risk factor for diseases other than stroke and ischemic heart disease. *Hypertension.* 2015;66:254–259. doi: 10.1161/HYPERTENSIONAHA.115.03480
3. Longstreth WT Jr, Bernick C, Manolio TA, Bryan N, Jungreis CA, Price TR. Lacunar infarcts defined by magnetic resonance imaging of 3660 elderly people: the Cardiovascular Health Study. *Arch Neurol.* 1998;55:1217–1225. doi: 10.1001/archneur.55.9.1217
4. Skoog I, Gustafson D. Update on hypertension and Alzheimer's disease. *Neural Res.* 2006;28:605–611. doi: 10.1179/016164106X130506
5. Humphrey JD. Mechanisms of vascular remodeling in hypertension. *Am J Hypertens.* 2021;34:432–441. doi: 10.1093/ajh/hpaa195

6. Bouhrara M, Spencer RG. Incorporation of nonzero echo times in the SPGR and bSSFP signal models used in mcDESPOT. *Magn Reson Med*. 2015;74:1227–1235. doi: 10.1002/mrm.25984
7. van Dalen JW, Mutsaerts HJ, Petr J, Caan MW, van Charante EPM, MacIntosh BJ, van Gool WA, Nederveen AJ, Richard E. Longitudinal relation between blood pressure, antihypertensive use and cerebral blood flow, using arterial spin labelling MRI. *J Cereb Blood Flow Metab*. 2021;41:1756–1766. doi: 10.1177/0271678X20966975
8. Sabisz A, Naumczyk P, Marcinkowska A, Graff B, Gasecki D, Glinska A, Witkowska M, Jankowska A, Konarzewska A, Kwela J, et al. Aging and hypertension - independent or intertwined white matter impairing factors? Insights from the quantitative diffusion tensor imaging. *Front Aging Neurosci*. 2019;11:35. doi: 10.3389/fnagi.2019.00035
9. Gons RA, de Laat KF, van Norden AG, van Oudheusden LJ, van Uden IW, Norris DG, Zwiers MP, de Leeuw F-E. Hypertension and cerebral diffusion tensor imaging in small vessel disease. *Stroke*. 2010;41:2801–2806. doi: 10.1161/STROKEAHA.110.597237
10. Nitkunan A, Charlton RA, McIntyre DJ, Barrick TR, Howe FA, Markus HS. Diffusion tensor imaging and MR spectroscopy in hypertension and presumed cerebral small vessel disease. *Magn Reson Med*. 2008;59:528–534. doi: 10.1002/mrm.21461
11. MacLulich AM, Ferguson KJ, Reid LM, Deary IJ, Starr JM, Seckl JR, Bastin ME, Wardlaw JM. Higher systolic blood pressure is associated with increased water diffusivity in normal-appearing white matter. *Stroke*. 2009;40:3869–3871. doi: 10.1161/STROKEAHA.109.547877
12. Song SK, Yoshino J, Le TQ, Lin SJ, Sun SW, Cross AH, Armstrong RC. Demyelination increases radial diffusivity in corpus callosum of mouse brain. *Neuroimage*. 2005;26:132–140. doi: 10.1016/j.neuroimage.2005.01.028
13. Pierpaoli C, Barnett A, Pajevic S, Chen R, Penix LR, Vitta A, Basser P. Water diffusion changes in Wallerian degeneration and their dependence on white matter architecture. *Neuroimage*. 2001;13(6 Pt 1):1174–1185. doi: 10.1006/nimg.2001.0765
14. Mohammadi S, Nagy Z, Moller HE, Symms MR, Carmichael DW, Josephs O, Weiskopf N. The effect of local perturbation fields on human DTI: characterisation, measurement and correction. *Neuroimage*. 2012;60:562–570. doi: 10.1016/j.neuroimage.2011.12.009
15. Kubicki M, Westin CF, Maier SE, Mamata H, Frumin M, Ersner-Hersfield H, Kikinis R, Jolesz FA, McCarley R, Shenton ME. Diffusion tensor imaging and its application to neuropsychiatric disorders. *Harv Rev Psychiatry*. 2002;10:324–336. doi: 10.1080/10673220216231
16. Bouhrara M, Spencer RG. Rapid simultaneous high-resolution mapping of myelin water fraction and relaxation times in human brain using BMC-mcDESPOT. *Neuroimage*. 2017;147:800–811. doi: 10.1016/j.neuroimage.2016.09.064
17. Bouhrara M, Cortina LE, Rejimon AC, Khattar N, Bergeron C, Bergeron J, Melvin D, Zukley L, Spencer RG. Quantitative age-dependent differences in human brainstem myelination assessed using high-resolution magnetic resonance mapping. *Neuroimage*. 2020;206:116307. doi: 10.1016/j.neuroimage.2019.116307
18. Alonso-Ortiz E, Levesque IR, Pike GB. MRI-based myelin water imaging: a technical review. *Magn Reson Med*. 2015;73:70–81. doi: 10.1002/mrm.25198
19. MacKay A, Whittall K, Adler J, Li D, Paty D, Graeb D. In vivo visualization of myelin water in brain by magnetic resonance. *Magn Reson Med*. 1994;31:673–677. doi: 10.1002/mrm.1910310614
20. Bouhrara M, Spencer RG. Improved determination of the myelin water fraction in human brain using magnetic resonance imaging through Bayesian analysis of mcDESPOT. *Neuroimage*. 2016;127:456–471. doi: 10.1016/j.neuroimage.2015.10.034
21. Deoni SC, Rutt BK, Peters TM. Rapid combined T1 and T2 mapping using gradient recalled acquisition in the steady state. *Magn Reson Med*. 2003;49:515–526. doi: 10.1002/mrm.10407
22. Gong Z, Bilgel M, Kiely M, Triebswetter C, Ferrucci L, Resnick SM, Spencer RG, Bouhrara M. Lower myelin content is associated with more rapid cognitive decline among cognitively unimpaired individuals [published online January 31, 2023]. *Alzheimer's Dement*. doi: 10.1002/alz.12968. <https://alz-journals.onlinelibrary.wiley.com/doi/10.1002/alz.12968>
23. Kiely M, Triebswetter C, Cortina LE, Gong Z, Alsameen MH, Spencer RG, Bouhrara M. Insights into human cerebral white matter maturation and degeneration across the adult lifespan. *Neuroimage*. 2022;247:118727. doi: 10.1016/j.neuroimage.2021.118727
24. Ferrucci L. The Baltimore Longitudinal Study of Aging (BLSA): a 50-year-long journey and plans for the future. *J Gerontol A Biol Sci Med Sci*. 2008;63:1416–1419. doi: 10.1093/gerona/63.12.1416
25. Shock NW, Gerontology Research Center (U.S.). *Normal human aging: the Baltimore longitudinal study of aging*. [Baltimore, Md.] Washington, D.C.: U.S. Dept. of Health and Human Services, Public Health Service, National Institutes of Health, National Institute on Aging For sale by the Supt. of Docs., U.S. G.P.O.; 1984. xix, 399, [34] p. p.
26. Bouhrara M, Alish JSR, Khattar N, Kim RW, Rejimon AC, Cortina LE, Qian W, Ferrucci L, Resnick SM, Spencer RG. Association of cerebral blood flow with myelin content in cognitively unimpaired adults. *BMJ Neurol Open*. 2020;2:e000053. doi: 10.1136/bmjno-2020-000053
27. Qian W, Khattar N, Cortina LE, Spencer RG, Bouhrara M. Nonlinear associations of neurite density and myelin content with age revealed using multicomponent diffusion and relaxometry magnetic resonance imaging. *Neuroimage*. 2020;223:117369. doi: 10.1016/j.neuroimage.2020.117369
28. Stollberger R, Wach P. Imaging of the active B1 field in vivo. *Magn Reson Med*. 1996;35:246–251. doi: 10.1002/mrm.1910350217
29. Bouhrara M, Spencer RG. Steady state double angle method for rapid B1 mapping. *Magn Reson Med*. 2019;82:189–201. doi: 10.1002/mrm.27708
30. Jenkinson M, Beckmann CF, Behrens TE, Woolrich MW, Smith SM. FSL. *Neuroimage*. 2012;62:782–790. doi: 10.1016/j.neuroimage.2011.09.015
31. Bouhrara M, Rejimon AC, Cortina LE, Khattar N, Bergeron CM, Ferrucci L, Resnick SM, Spencer RG. Adult brain aging investigated using BMC-mcDESPOT-based myelin water fraction imaging. *Neurobiol Aging*. 2020;85:131–139. doi: 10.1016/j.neurobiolaging.2019.10.003
32. Bouhrara M, Khattar N, Elango P, Resnick SM, Ferrucci L, Spencer RG. Evidence of association between obesity and lower cerebral myelin content in cognitively unimpaired adults. *Int J Obes (Lond)*. 2021;45:850–859. doi: 10.1038/s41366-021-00749-x
33. Bouhrara M, Reiter DA, Bergeron CM, Zukley LM, Ferrucci L, Resnick SM, Spencer RG. Evidence of demyelination in mild cognitive impairment and dementia using a direct and specific magnetic resonance imaging measure of myelin content. *Alzheimers Dement*. 2018;14:998–1004. doi: 10.1016/j.jalz.2018.03.007
34. Walker KA, Duggan MR, Gong Z, Dark HE, Laporte JP, Faulkner ME, An Y, Lewis A, Moghekar AR, Resnick SM, et al. MRI and fluid biomarkers reveal determinants of myelin and axonal loss with aging. *Ann Clin Transl Neurol*. 2023;10:397–407. doi: 10.1002/acn3.51730
35. Knopik DS, Mosley TH, Catellier DJ, Sharrett AR; Atherosclerosis Risk in Communities (ARIC) Study. Cardiovascular risk factors and cerebral atrophy in a middle-aged cohort. *Neurology*. 2005;65:876–881. doi: 10.1212/01.wnl.0000176074.09733.a8
36. Bouhrara M, Reiter DA, Celik H, Fishbein KW, Kijowski R, Spencer RG. Analysis of mcDESPOT- and CPMG-derived parameter estimates for two-component nonexchanging systems. *Magn Reson Med*. 2016;75:2406–2420. doi: 10.1002/mrm.25801
37. Bouhrara M, Kim RW, Khattar N, Qian W, Bergeron CM, Melvin D, Zukley LM, Ferrucci L, Resnick SM, Spencer RG. Age-related estimates of aggregate g-ratio of white matter structures assessed using quantitative magnetic resonance neuroimaging. *Hum Brain Mapp*. 2021;42:2362–2373. doi: 10.1002/hbm.25372
38. Khattar N, Triebswetter C, Kiely M, Ferrucci L, Resnick SM, Spencer RG, Bouhrara M. Investigation of the association between cerebral iron content and myelin content in normative aging using quantitative magnetic resonance neuroimaging. *Neuroimage*. 2021;239:118267. doi: 10.1016/j.neuroimage.2021.118267
39. Triebswetter C, Kiely M, Khattar N, Ferrucci L, Resnick SM, Spencer RG, Bouhrara M. Differential associations between apolipoprotein E alleles and cerebral myelin content in normative aging. *Neuroimage*. 2022;251:118988. doi: 10.1016/j.neuroimage.2022.118988
40. Bouhrara M, Cortina LE, Khattar N, Rejimon AC, Ajamu S, Cezayirli DS, Spencer RG. Maturation and degeneration of the human brainstem across the adult lifespan. *Aging (Albany NY)*. 2021;13:14862–14891. doi: 10.18632/aging.203183
41. Kiely M, Triebswetter C, Gong Z, Laporte JP, Faulkner ME, Akhonda M, Alsameen MH, Spencer RG, Bouhrara M. Evidence of an association between cerebral blood flow and microstructural integrity in normative aging using a holistic MRI approach [published online November 3, 2022]. *J Magn Reson Imaging*. doi: 10.1002/jmri.28508. <https://onlinelibrary.wiley.com/doi/10.1002/jmri.28508>
42. Cortina LE, Kim RW, Kiely M, Triebswetter C, Gong Z, Alsameen MH, Bouhrara M. Cerebral aggregate g-ratio mapping using magnetic resonance relaxometry and diffusion tensor imaging to investigate sex and age-related differences in white matter microstructure. *Magn Reson Imaging*. 2022;85:87–92. doi: 10.1016/j.mri.2021.10.019
43. Bouhrara M, Rejimon AC, Cortina LE, Khattar N, Bergeron CM, Ferrucci L, Resnick SM, Spencer RG. Adult brain aging investigated using

- BMC-mcDESPOT based myelin water fraction imaging. *Neurobiol Aging*. 2019. doi: 10.1016/j.neurobiolaging.2019.10.003
44. Bouhrara M, Cortina LE, Rejimon AC, Khattar N, Bergeron C, Bergeron J, Bergeron J, Melvin D, Zukley L, Spencer RG. Quantitative age-dependent differences in human brainstem myelination assessed using high-resolution diffusion magnetic resonance mapping. *Neuroimage*. 2020;206:116307 doi: 10.1016/j.neuroimage.2019.116307
 45. Faulkner ME, Laporte JP, Gong Z, Akhonda MABS, Triebswetter C, Kiely M, Palchamy E, Spencer RG, Bouhrara M. Lower myelin content is associated with lower gait speed in cognitively unimpaired adults [published online March 5, 2023]. *J Gerontol*. doi:10.1093/gerona/glad080.https://academic.oup.com/biomedgerontology/advance-article/doi/10.1093/gerona/glad080/7069863
 46. Basser PJ, Jones DK. Diffusion-tensor MRI: theory, experimental design and data analysis - a technical review. *NMR Biomed*. 2002;15:456-467. doi: 10.1002/nbm.783
 47. Brant LJ, Ferrucci L, Sheng SL, Concin H, Zonderman AB, Kelleher CC, Longo DL, Ulmer H, Strasak AM. Gender differences in the accuracy of time-dependent blood pressure indices for predicting coronary heart disease: a random-effects modeling approach. *Genet Med*. 2010;7:616-627. doi: 10.1016/j.genm.2010.11.005
 48. Benjamini Y. Discovering the false discovery rate. *J Royal Stat Soc*. 2010;72:405-416. doi: 10.1111/j.1467-9868.2010.00746.x
 49. Benjamini Y, Hochberg Y. Controlling the false discovery rate: a practical and powerful approach to multiple testing. *J Royal Stat Soc*. 1995;57:289-300. doi: 10.1111/j.2517-6161.1995.tb02031.x
 50. Huang L, Ling XY, Liu SR. Diffusion tensor imaging on white matter in normal adults and elderly patients with hypertension. *Chin Med J (Engl)*. 2006;119:1304-1307.
 51. Pasi M, van Uden IW, Tuladhar AM, de Leeuw FE, Pantoni L. White matter microstructural damage on diffusion tensor imaging in cerebral small vessel disease: clinical consequences. *Stroke*. 2016;47:1679-1684. doi: 10.1161/STROKEAHA.115.012065
 52. Suri S, Topiwala A, Chappell MA, Okell TW, Zsoldos E, Singh-Manoux A, Kivimäki M, Mackay CE, Ebmeier KP. Association of midlife cardiovascular risk profiles with cerebral perfusion at older ages. *JAMA Netw Open*. 2019;2:e195776. doi: 10.1001/jamanetworkopen.2019.5776
 53. Pires PW, Dams Ramos CM, Matin N, Dorrance AM. The effects of hypertension on the cerebral circulation. *Am J Physiol Heart Circ Physiol*. 2013;304:H1598-H1614. doi: 10.1152/ajpheart.00490.2012
 54. Scuteri A, Nilsson PM, Tzourio C, Redon J, Laurent S. Microvascular brain damage with aging and hypertension: pathophysiological consideration and clinical implications. *J Hypertens*. 2011;29:1469-1477. doi: 10.1097/HJH.0b013e328347cc17
 55. Oh YS. Arterial stiffness and hypertension. *Clin Hypertens*. 2018;24:17. doi: 10.1186/s40885-018-0102-8
 56. Safar ME, Asmar R, Benetos A, Blacher J, Boutouyrie P, Lacolley P, Laurent S, London G, Pannier B, Protogerou A, et al; French Study Group on Arterial Stiffness. Interaction between hypertension and arterial stiffness. *Hypertension*. 2018;72:796-805. doi: 10.1161/HYPERTENSIONAHA.118.11212
 57. Bouhrara M, Triebswetter C, Kiely M, Bilgel M, Dolui S, Erus G, Meirelles O, Bryan NR, Detre JA, Launer LJ. Association of cerebral blood flow with longitudinal changes in cerebral microstructural integrity in the coronary artery risk development in young adults (CARDIA) study. *JAMA Netw Open*. 2022;5:e2231189. doi: 10.1001/jamanetworkopen.2022.31189
 58. Costa-Mattoli M, Walter P. The integrated stress response: from mechanism to disease. *Science*. 2020;368:6489. doi: 10.1126/science.aat5314
 59. Rosko L, Smith VN, Yamazaki R, Huang JK. Oligodendrocyte bioenergetics in health and disease. *Neuroscientist*. 2019;25:334-343. doi: 10.1177/1073858418793077
 60. Lyons SA, Kettenmann H. Oligodendrocytes and microglia are selectively vulnerable to combined hypoxia and hypoglycemia injury in vitro. *J Cereb Blood Flow Metab*. 1998;18:521-530. doi: 10.1097/00004647-199805000-00007
 61. Mohammadi MT, Dehghani GA. Acute hypertension induces brain injury and blood-brain barrier disruption through reduction of claudins mRNA expression in rat. *Pathol Res Pract*. 2014;210:985-990. doi: 10.1016/j.prp.2014.05.007
 62. Bajwa E, Klegeris A. Neuroinflammation as a mechanism linking hypertension with the increased risk of Alzheimer's disease. *Neural Regen Res*. 2022;17:2342-2346. doi: 10.4103/1673-5374.336869
 63. Gons RA, van Oudheusden LJ, de Laat KF, van Norden AG, van Uden IW, Norris DG, Zwiers MP, van Dijk E, de Leeuw F-E. Hypertension is related to the microstructure of the corpus callosum: the RUN DMC study. *J Alzheimers Dis*. 2012;32:623-631. doi: 10.3233/JAD-2012-121006
 64. de Groot M, Ikram MA, Akoudad S, Krestin GP, Hofman A, van der Lugt A, Niessen WJ, Vernooij MW. Tract-specific white matter degeneration in aging: the Rotterdam Study. *Alzheimers Dement*. 2015;11:321-330. doi: 10.1016/j.jalz.2014.06.011
 65. Maillard P, Seshadri S, Beiser A, Himali JJ, Au R, Fletcher E, Carmichael O, Wolf PA, DeCarli C. Effects of systolic blood pressure on white-matter integrity in young adults in the Framingham Heart Study: a cross-sectional study. *Lancet Neurol*. 2012;11:1039-1047. doi: 10.1016/S1474-4422(12)70241-7
 66. Johnson B, Zhang K, Gay M, Neuberger T, Horovitz S, Hallett M, Sebastianelli W, Slobounov S. Metabolic alterations in corpus callosum may compromise brain functional connectivity in MTBI patients: an 1H-MRS study. *Neurosci Lett*. 2012;509:5-8. doi: 10.1016/j.neulet.2011.11.013
 67. Kumral E, Bayulkem G. Spectrum of single and multiple corona radiata infarcts: clinical/MRI correlations. *J Stroke Cerebrovasc Dis*. 2003;12:66-73. doi: 10.1053/j.scd.2003.11
 68. Goldstein A, Covington BP, Mahabadi N, Mesfin FB. *Neuroanatomy, Corpus Callosum*. StatPearls: Treasure Island (FL); 2022.
 69. McQueen J, Reimer MM, Holland PR, Manso Y, McLaughlin M, Fowler JH, Horsburgh K. Restoration of oligodendrocyte pools in a mouse model of chronic cerebral hypoperfusion. *PLoS One*. 2014;9:e87227. doi: 10.1371/journal.pone.0087227
 70. Dewar D, Underhill SM, Goldberg MP. Oligodendrocytes and ischemic brain injury. *J Cereb Blood Flow Metab*. 2003;23:263-274. doi: 10.1097/01.WCB.0000053472.41007.F9
 71. Beason-Held LL, Moghekar A, Zonderman AB, Kraut MA, Resnick SM. Longitudinal changes in cerebral blood flow in the older hypertensive brain. *Stroke*. 2007;38:1766-1773. doi: 10.1161/STROKEAHA.106.477109
 72. Khachaturian AS, Zandi PP, Lyketsos CG, Hayden KM, Skoog I, Norton MC, Tschanz JT, Mayer LS, Welsh-Bohmer KA, Breitner JCS. Antihypertensive medication use and incident Alzheimer disease: the Cache County Study. *Arch Neurol*. 2006;63:686-692. doi: 10.1001/archneur.63.5.noc60013
 73. Shah NS, Vidal JS, Masaki K, Petrovitch H, Ross GW, Tilley C, DeMattos RB, Tracy RP, White LR, Launer LJ. Midlife blood pressure, plasma beta-amyloid, and the risk for Alzheimer disease: the Honolulu Asia Aging Study. *Hypertension*. 2012;59:780-786. doi: 10.1161/HYPERTENSIONAHA.111.178962
 74. Power MC, Weuve J, Gagne JJ, McQueen MB, Viswanathan A, Blacker D. The association between blood pressure and incident Alzheimer disease: a systematic review and meta-analysis. *Epidemiology*. 2011;22:646-659. doi: 10.1097/EDE.0b013e31822708b5